Supporting Information

A Combined SECM and Electrochemical AFM Approach to Probe Interfacial Processes Affecting Molecular Reactivity at Redox Flow Battery Electrodes

Tylan Watkins,[†,a,d] Dipobrato Sarbapalli,[†,b,d] Michael J. Counihan,[†,b,d] Andrew S. Danis,[b,d] Jingjing Zhang,[c,d] Lu Zhang,[c,d] Kevin R. Zavadil,[a,d,*] Joaquín Rodríguez-López[b,d,*]

[a] Material, Physical and Chemical Sciences Center, Sandia National Laboratories, Albuquerque, NM 87185, USA

[b] Department of Chemistry, University of Illinois at Urbana-Champaign, 600 South Mathews Avenue, Urbana, IL 61801, USA

[c] Chemical Sciences and Engineering Division, Argonne National Laboratory, 9700 South Cass Avenue, Argonne, IL 60439, USA

[d] Joint Center for Energy Storage Research, Argonne, IL 60439, USA

Table of Contents:

I. Materials and Methods:

A. Materials:

All chemicals were purchased from commercial sources and used as received. Propylene carbonate (PC, anhydrous, 99.7%), lithium tetrafluoroborate ($LiBF_4$, 98%), ferrocene (98%), acetone (99.5%), isopropyl alcohol (IPA 99.5%), glacial acetic acid (99.5%), and ethylenediaminetetraacetic acid disodium salt dihydrate ($Na_2EDTA{\cdot}2H_2O$, 99.0%), Poly (Bisphenol A carbonate), with an average M_w of around 45,000, were all purchased from Sigma-Aldrich. Lithium bis(trifluoromethylsulfonyl)imide (LiTFSI, 99.99%) was purchased from Osilla. Copper foil, 25μm thick, was purchased from Alfa Aesar. Copper etchant was purchased from Transene Company. SiO_2/Si wafer (3 in. B-doped P-type Si wafer with 300 nm wet thermal oxide) was purchased from University Wafer. C1 and C7 were synthesized via previously established procedures (see main text for references).

B. Graphene Synthesis:

Graphene was grown through chemical vapor deposition (CVD) on pretreated copper foil catalyst closely following previous procedures.[1,2] The Cu foil was treated in acetone (10 s), water (10 s), glacial acetic acid (10 min), water (10 s), acetone (10 s), and IPA (10 s) to remove any surface oxides. The Cu foil was then mounted in CVD furnace (Lindberg Blue M, Thermo Scientific) for graphene growth. A methodology from previously reported atmosphere pressure CVD graphene synthesis,[1] with no annealing step and growth at 960 °C, 10 sccm CH_4 and 30 sccm H_2 for 5 min was employed to obtain the multi-layer graphene (MLG) substrates. Single layer graphene was procured commercially from GrollTex.

C. Graphene Transfer:

CVD grown graphene was transferred on SiO_2/Si wafer and glass coverslips (for optical transmittance characterization) through a wet transfer method.[3] After graphene growth, one side of the Cu foil with graphene was protected with 1 layer of Poly(Bisphenol A carbonate), henceforth referred as polycarbonate, via spin-coating at 3000 rpm for 30 s. Post coating, MLG from the other side was removed using scotch tape. Oxygen plasma was used to remove SLG from the other side of the Cu foil (Harrick Plasma, 40 W power, 1 torr O_2 pressure, 3 min exposure). The protected graphene was floated on top of Cu etchant for 1 h at 40°C to remove Cu foil beneath the graphene. The floating graphene/polycarbonate sheet went through 4 rinse steps with DI water, 1 h treatment with 0.1 M Na_2EDTA aqueous solution, and 4 rinse steps with DI water again to fully remove any metal residue. The clean graphene/polycarbonate sheet was finally transferred onto the desired substrate and blow dried under argon, and subsequently kept in a vacuum desiccator overnight. After drying, samples were immersed in chloroform overnight to remove polycarbonate protecting layer, and then rinsed with acetone and IPA twice. Samples were used after blow drying IPA from the final rinse step with argon.

D. Graphene Characterization:

The CVD grown graphene was characterized through SEM, Raman and transmittance microscopy. The transmittance of graphene to radiation between 500-700nm wavelengths is known to be 2.3% per layer.[4] Transmittance micrographs were obtained at 561nm using a Leica SP8 Confocal Microscope, and it was assumed that each layer absorbs 2.3% of the light. Each individual pixel from the micrograph were individually converted to yield a no. of layers, and therefore, the resulting image now displays the spatial distribution of no. of layers of graphene. Raman spectra and images were collected using a Nanophoton Laser Raman Microscope (RAMAN-11, Japan). Scanning electron microscopy (SEM) was performed on a Hitachi S4700 field emission.

SEM micrographs (Manuscript Figure Ci and Cii) reveal full coverage of graphene on Si wafer with minimal tears. The morphology and structure of graphene is in line with what is observed for atmospheric pressure CVD synthesis of graphene.[5] There are clear dark bands of multi-layered graphene, with the lighter area around the bands clearly having fewer layers.

Raman spectro-microscopy (Figure S1) confirms that the dark bands are multi-layered graphene. The lighter regions are observed to have a 2D/G peak intensity ratio of 1 and >1, which is characteristic of bilayer (BLG) and single layer graphene (SLG) respectively.

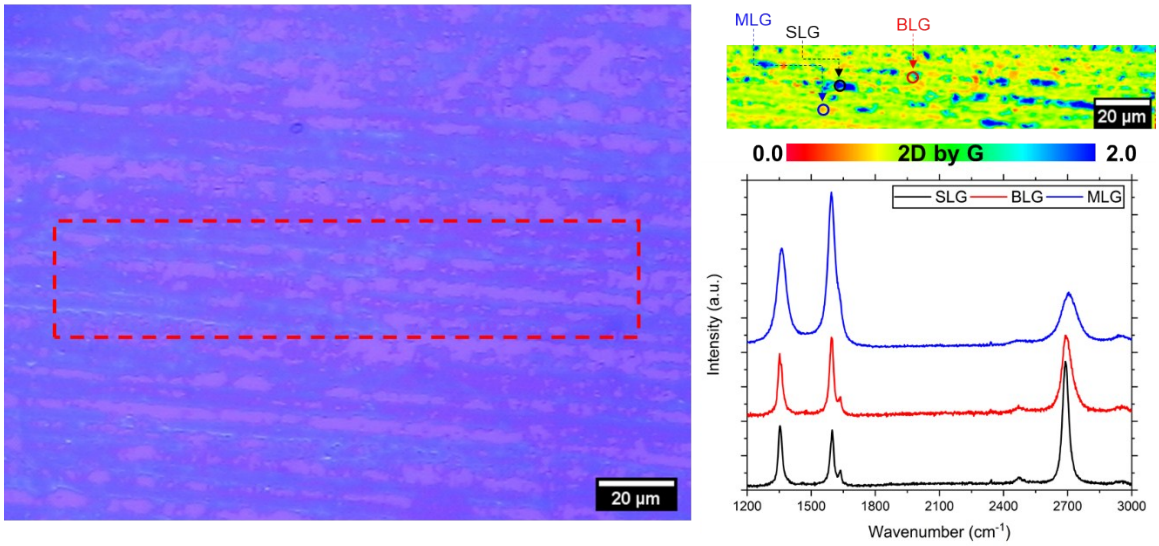

Figure S1: Raman 2D/G peak mapping (top right) showing spatial distribution of MLG, BLG and SLG regions within the red dotted region on optical micrograph (left) of CVD-grown graphene substrates

Transmittance micrographs in Figure S2 results also show the similar results, with most of the graphene appearing to be 5-15 layers thick. Single and bi-layer regions are also observed (blue areas) along with thicker graphene areas varying from 15-20 layers.

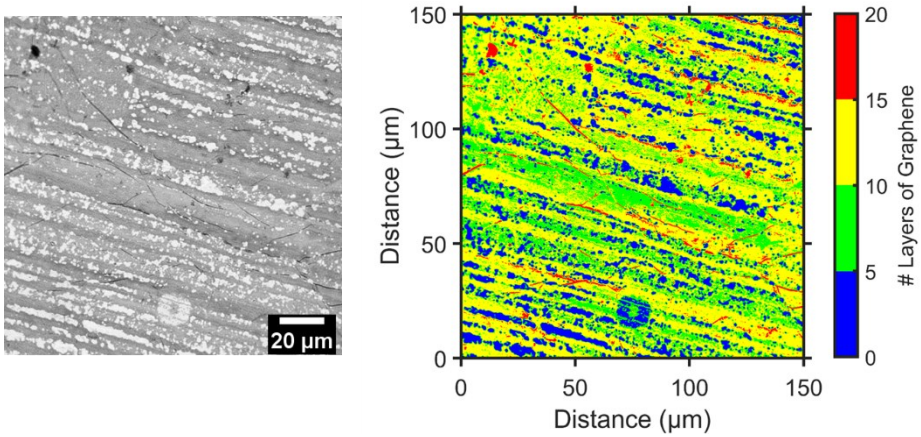

Figure S2: Transmittance micrograph (left) of CVD graphene, and resulting number of graphene layers (right) after image analysis

E. HOPG Edge Sample Preparation:

Highly oriented pyrolytic graphite (HOPG, brand grade SPI-2, SPI) and solid slabs of flexible low-density polyethylene (LDPE, 12" x 12" x 1/4"sheet fromMcMaster-Carr) were used for edge plane HOPG preparation, following previous work in our group.[6] HOPG sheets were peeled off using conductive Cu tape and then sealed between two pieces of LDPE. Subsequently, the setup was kept in a vacuum oven at 80°C for 2 hours and cooled under ambient air. The edge plane was then exposed by cutting and polishing with 5µm and 1µm SiC paper. This procedure resulted in the HOPG surface being at a lower height than the adjacent LDPE blocks as shown in Figure S3. Therefore, we resorted to two methods to estimate HOPG Edge – tip distance.

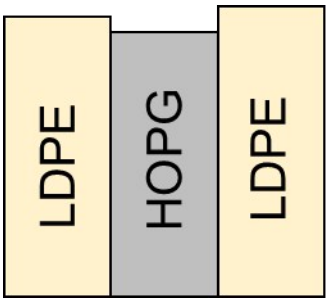

Figure S3: Schematic of sample cross section for HOPG Substrate

F: HOPG Height Measurements:

1: Using SECM Approach Curves

We approached to 150% positive feedback over the HOPG Edge plane as shown in Figure S4's inset. From our i/i_∞ images, where we positioned the tip to 60% negative feedback over LDPE, the approximate positive feedback over HOPG edge was around 110% (Figure S4). Therefore, using the positive feedback approach curve, we estimated that this feedback occurs at tip-substrate

separation of ≈2.6L (Figure S4). Positive feedback approach curve was fit using theoretical equations laid down by Cornut and Lefrou,[7] modified to account for shifts in x and y axes.

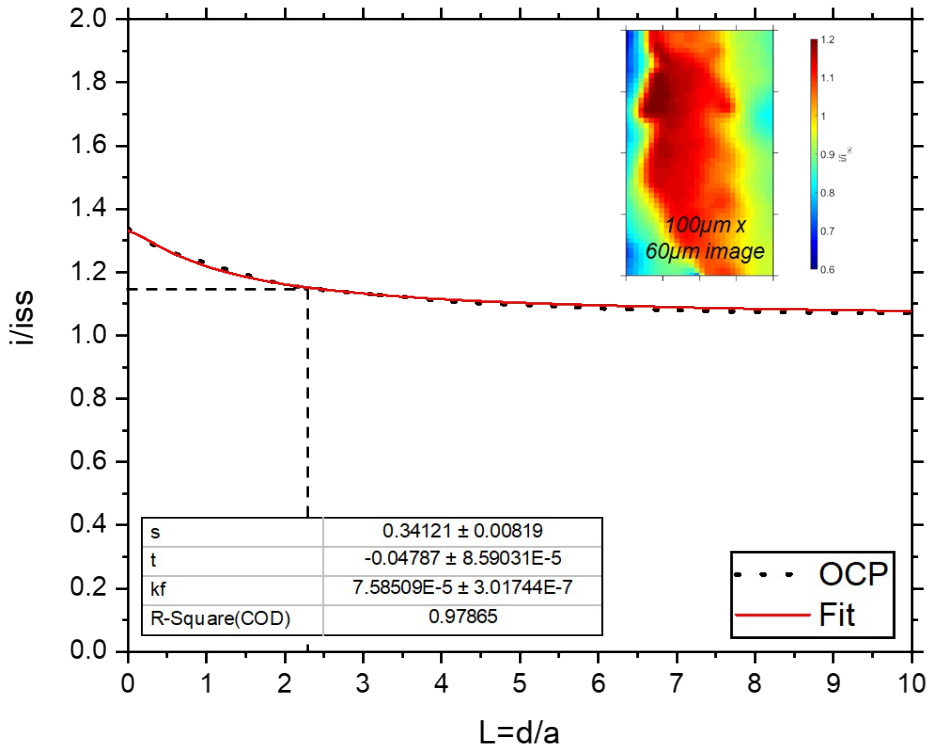

Figure S4: Positive feedback approach to 150% (dotted line) reveal tip-substrate distance to be ≈2.6L for a i/i_{ss} (i_{ss} is same as i_∞) of 1.1. Red trace is theoretical fit. Note, the fit parameter s is the tip to substrate distance for 150% positive approach, which is added to the 2.3L for getting actual tip-substrate distance

2: Using Optical Profilometry

We used a Keyence VK-X1000 3D Laser Scanning Confocal Microscope to take a profile of the sample substrate after analysis, shown in Figure S5. We take the average heights along every single horizontal strip of pixels and plot this average height as a function of distance in the vertical axis, as shown in Figure S5. This reveals the HOPG edge to be slightly depressed by around 1.8-2.4µm. This is equivalent to around 1L to 1.4L for a tip of radius ≈1.75µm. Since the tip was estimated to be 1L from HOPG edge, this means that the tip to HOPG edge distance was around 2-2.4L, quite consistent with the result from positive approach feedback curves. Therefore, we resorted to calculating our k_f values at a tip-substrate distance of 2.6L for the HOPG edge samples.

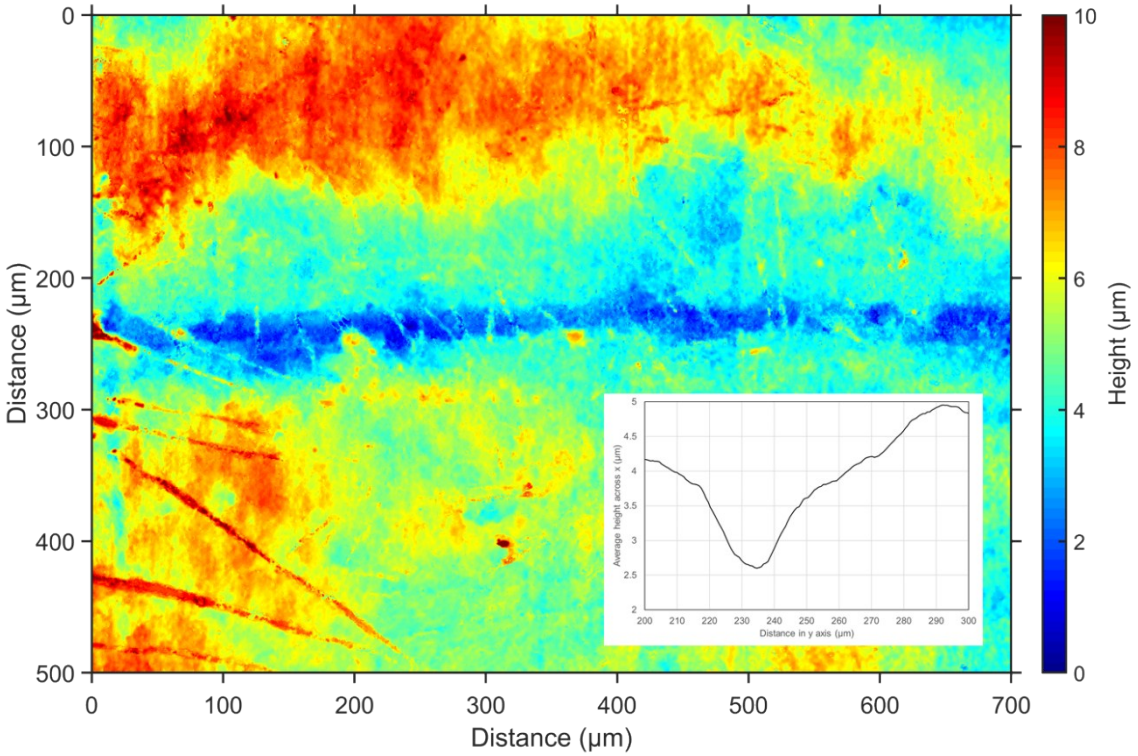

Figure S5: Profilometry image of edge plane HOPG after testing, with average heights along x as a function of distance along y presented inset. The HOPG edge is around 1.8-2.4µm below the surrounding LDPE (within a 60µm distance, the same as that of our SECM image)

G. SECM Electrochemistry Protocol:

Cyclic voltammetry (potential sweep) and chronoamperometry (potential step) was used to cycle all substrates. All voltammograms were performed at a scan rate of 20 mV/s. In some cases, we could not reach mass transfer limited currents despite biasing to overpotentials >200-400 mV owing to solution resistance arising from the distance between reference and substrates. Chronoamperometry was performed at a mass transfer limited oxidizing potential and reduction at 0V w.r.t silver wire quasi-reference for 60s at each step. 5 sets of chronoamperometry was performed. After the 1+25 cycles of CV and 5 sets of chronoamperometry, we performed an additional potential step experiment wherein we bias the substrate at 0V for ≈30 and 10 mins respectively. This was done to reduce the oxidized catholyte species generated by the cycling experiments and preserve the concentration of catholyte species started out with initially.

Before every set of SECM images, we took steady state current (i_∞) measurements by biasing the UME tip to at least 200 mV of oxidizing overpotential, at a height of 50 µm above the substrates. The same tip potential was used for approach curves and SECM feedback imaging. Quiet time was set for 30 s, same as all SECM and approach curve measurements. The current measurement was recorded for 30 s at 0.1 s sampling interval and averaged out to get the steady state measurement. These steady state currents were subsequently used to generate normalized SECM images.

II. Macrodisk Electrochemistry:

A. C1, C6 (2,5-dimethyl-1,4-dialkoxybenzene), and C7 Comparison in $LiBF_4$:

1. Cyclic Voltammetry on Pt and GC Working Electrodes:

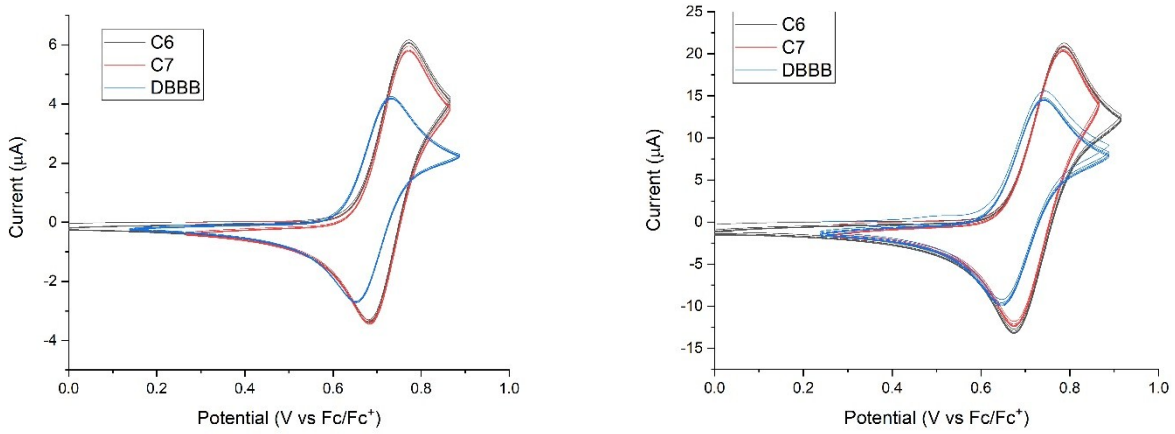

Figure S6: Macrodisk electrochemistry comparing C1 (blue trace), C6 (black trace), and C7 (red trace) first oxidation electrochemistry. 5 mM solutions of target analyte performed on a 2 mm diameter Pt disk working electrode (left) and a 3 mm glassy carbon diameter working electrode (right). Solutions were made of 5 mM target analyte 0.1 M $LiBF_4$ in PC and evaluated using cyclic voltammetry to probe the first Faradaic oxidation at a scan rate of 10 mV/s for all samples. Electrochemistry was performed using a three electrode system with either Pt or glassy carbon working electrode, metal polypyrrole quasi-reference electrode (ppy/ppy^+),[8] and a Pt counter electrode. Macrodisk electrochemistry displays the influence of faster diffusion coefficients of C6 and C7 with higher peak currents than C1, and the influence of less substitution with C6 and C7 having higher oxidation potentials than C1.

2. C1, C6, and C7 Scan Rate Analysis with Simulation:

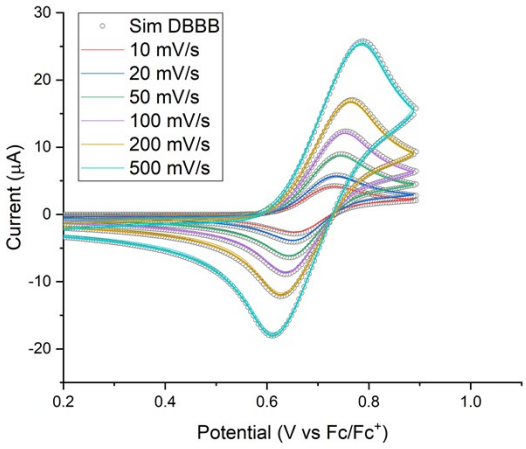

A)

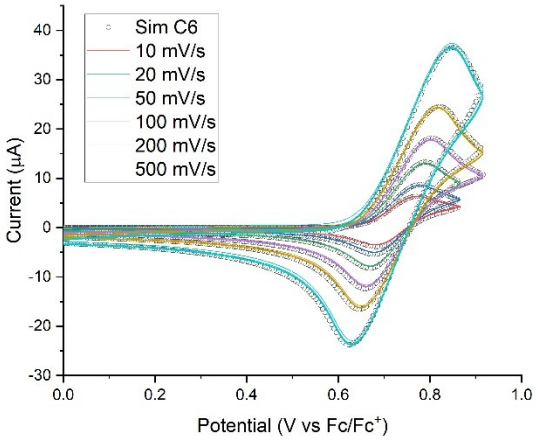

B)

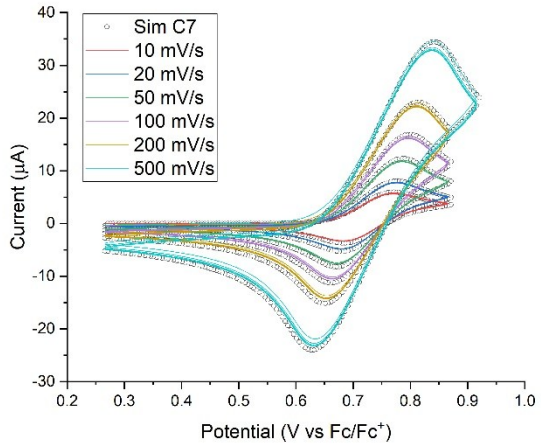

C)

Figure S7: Scan rate analysis performed on C1 (A), C6 (B), and C7 (C) overlaid with simulation (circles) following the progression of scan rates. A scan rate analysis was performed using a three-electrode system with a Pt working electrode, ppy/ppy$^+$ reference electrode, and a Pt counter electrode and varying the scan rate of cyclic voltammograms from 10 mV/s up to 500 mV/s. The simulations were generated using Digi-Elch software and a fixed solution resistance of 1800 Ω and fixed capacitance of 0.5 µF for all three analytes.

3. Electrochemical Stability of C7:

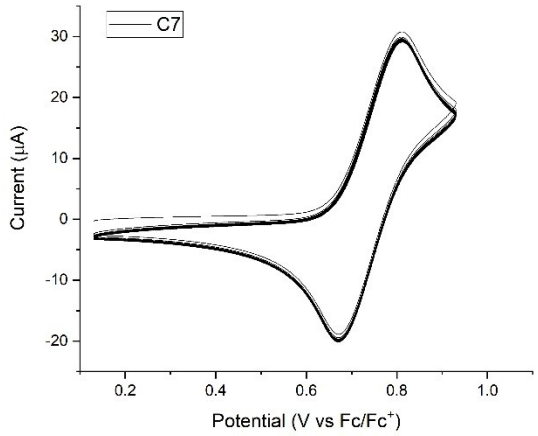

Figure S8: C7 stability testing using macro electrode. Cyclic voltammetry performed on a solution of 5 mM C7 and 0.1 M $LiBF_4$ in PC ramping the potentials from 0.65 V to 1.45 V to 0.65 V for 100 cycles at a scan rate of 25 mV/s. The three electrode setup used consisted of a 3 mm glassy

carbon working electrode, a reference electrode of ppy/ppy$^+$, and a Pt counter electrode. No appreciable change in current was observed for the faradaic current of C7 over 100 cycles.

B. C1 and C7 Comparison in LiTFSI:

1. Cyclic Voltammetry on GC Working Electrodes:

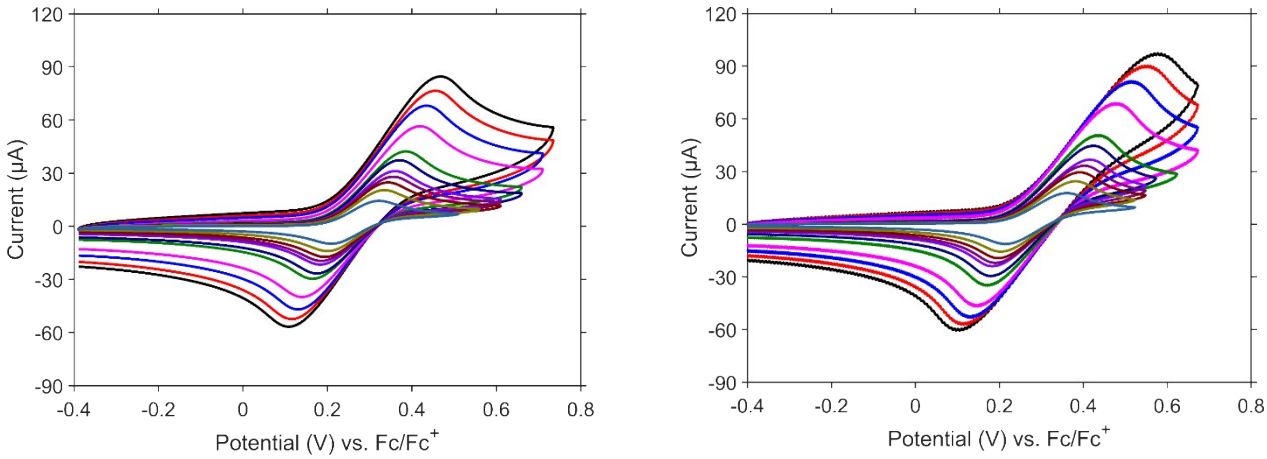

Figure S9: Macrodisk electrochemistry comparing C1 (left), and C7 (right) first oxidation process using 0.1 M LiTFSI in PC. Electrochemistry was performed using a three-electrode system with a 3mm glassy carbon working electrode, Ag/AgCl reference electrode (potentials adjusted to Fc/Fc$^+$), and a Pt counter electrode. Scan rates used were 500, 400, 300, 200, 100, 75, 50, 40, 30, 20, 10 mV/s.

2. C1 and C7 Scan Rate Analysis with Simulation:

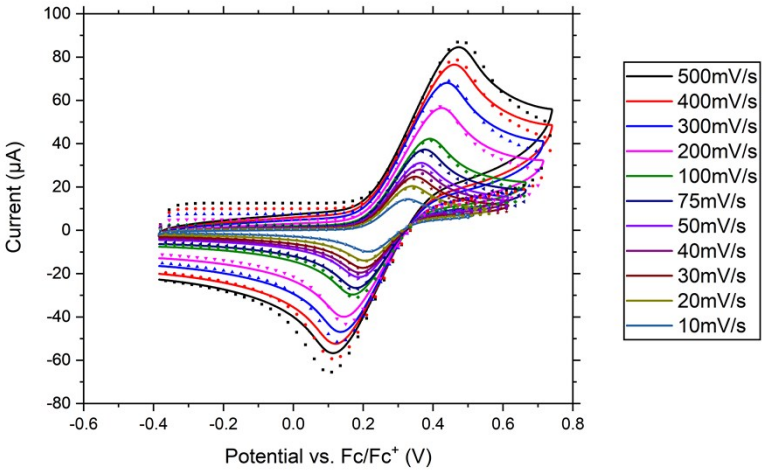

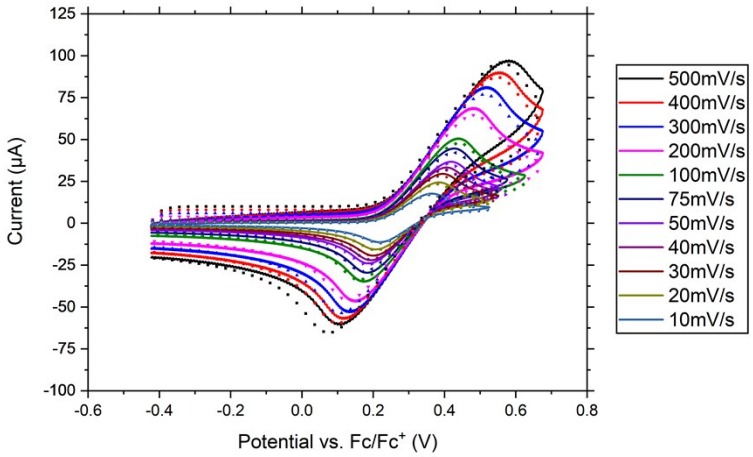

Figure S10: Comparison of scan rate analysis with 5 mM C1 (top) and 5 mM C7 (bottom) in 0.1 M LiTFSI with simulation (dotted traces). Simulations were generated using Digi-Elch software and a solution resistance of 1500 Ω and 2000 Ω (for C1 and C7 respectively) and fixed capacitance of 0.25 μF for both analytes.

C: Summary of Electrochemical Parameters Used to Generate Simulations

Electrochemistry parameters used to generate the simulations for C1, C6, and C7 were:

Parameter	C1		C6	C7	
Electrolyte	$LiBF_4$	LiTFSI	$LiBF_4$	$LiBF_4$	LiTFSI
Diffusion Coefficient (cm^2/s)	1.08×10^{-6}	2.3×10^{-6}	2.25×10^{-6}	2.23×10^{-6}	3.6×10^{-6}
Formal Potential (V vs Fc/Fc^+)	0.693	0.685	0.726	0.726	0.724
Heterogeneous Rate Constant, k^0 (m/s)*	1.3×10^{-4}	1.0×10^{-4}	1.0×10^{-4}	1.5×10^{-4}	1.0×10^{-4}
Transfer Coefficient	0.50	0.50	0.53	0.53	0.50

*These values were used exclusively as model inputs for DigiElch. The heterogeneous rate constants used to reproduce the macroelectrode cyclic voltammetry are understood to be empirically limited in their accuracy. This stems from contributions of solution resistance, capacitance, and mass transport preventing the observation and subsequent fitting of faster heterogeneous rate constants.

III. SECM: Comparing C1 and C7 on MLG with $LiBF_4$

A. C1 – Biased Substrate's CVs and CAs

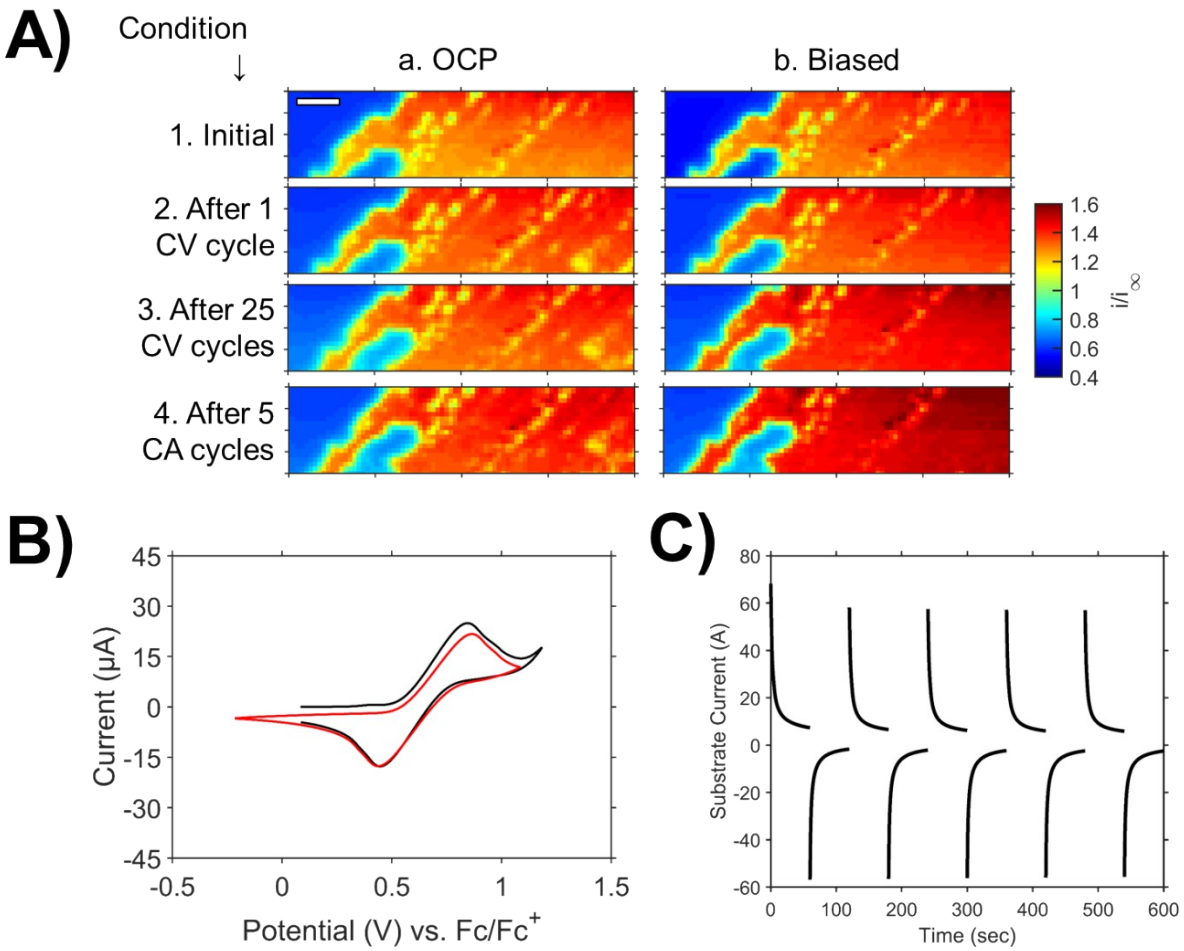

Figure S11: A) Normalized SECM images of a MLG electrode using 5 mM C1 as catholyte mediator in 0.1 M $LiBF_4$ electrolyte in PC; image scale bars are 20 μm. Images were taken with the substrate electrode: (i) at the initial condition before substrate biasing, (ii) after one substrate CV, (iii) after 25 more substrate CVs, and (iv) after five sets of oxidative then reductive chronoamperograms. The probe was biased at 0.88 V vs. Fc/Fc^+, and the substrate was either at a) OCP or b) biased to -0.22 V vs. Fc/Fc^+. B) Cyclic voltammograms with the MLG substrate. The black trace is the first cycle and red trace is the 26th total cycle. C) Chronoamperometry with MLG substrate using an oxidation potential of 1.08 V vs. Fc/Fc^+ and reduction potential of -0.22 V vs Fc/Fc^+.

B. C7 – Biased Substrate's CVs and CAs

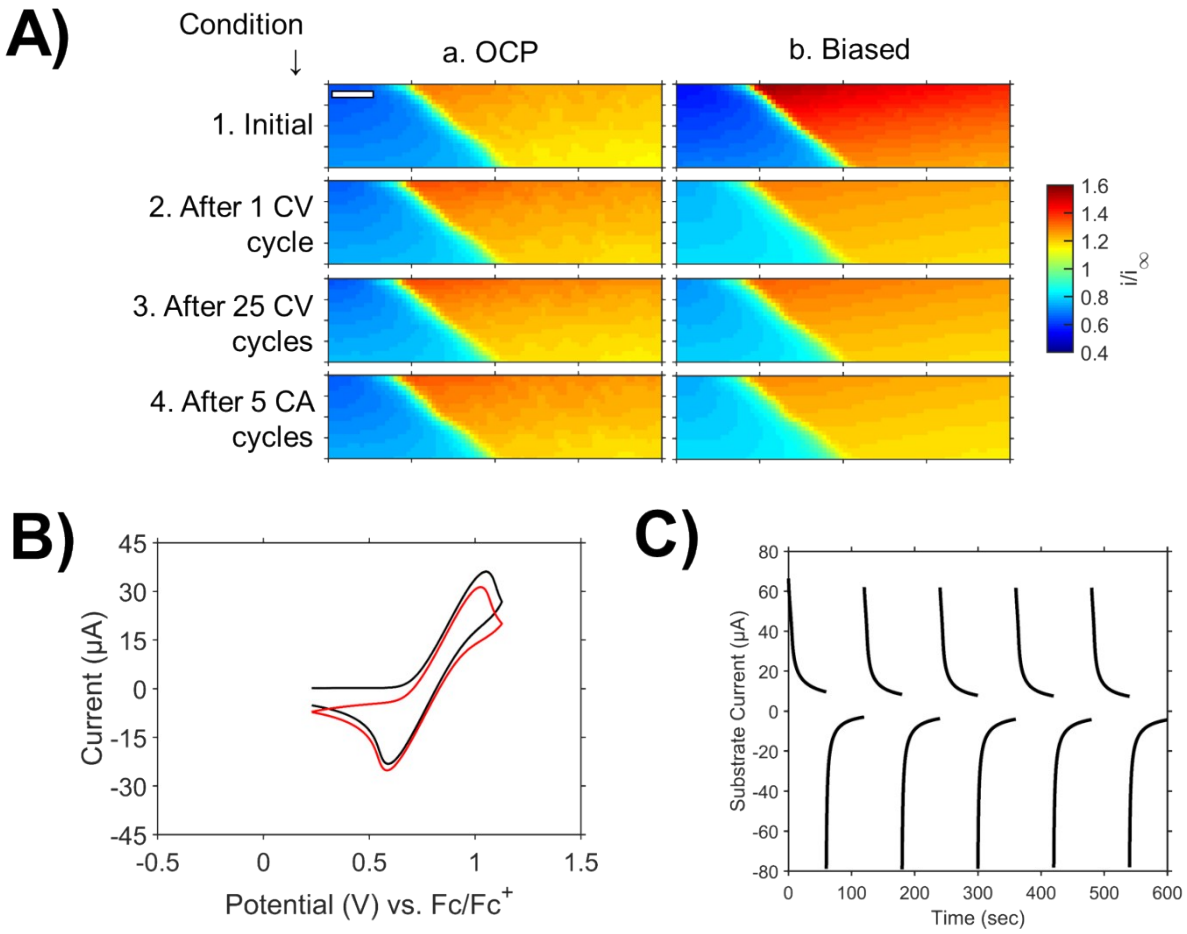

Figure S12: A) Normalized SECM images of a MLG electrode using 5 mM C7 as catholyte mediator in 0.1 M $LiBF_4$ electrolyte in PC; image scale bars are 20 μm. Images were taken with the substrate electrode: (i) at the initial condition before substrate biasing, (ii) after one substrate CV, (iii) after 25 more substrate CVs, and (iv) after five sets of oxidative then reductive chronoamperograms. The probe was biased at 0.926 V vs. Fc/Fc^+, and the substrate was either at (a) OCP or (b) biased to -0.17 V vs. Fc/Fc^+. B) Cyclic voltammograms with MLG substrate. The black trace is the first cycle and red trace is the 26^{th} total cycle. C) Chronoamperometry with MLG substrate using an oxidation potential of 1.13 V vs. Fc/Fc^+ and reduction potential of -0.17 V vs Fc/Fc^+.

C. TCNQ + C1 Imaging

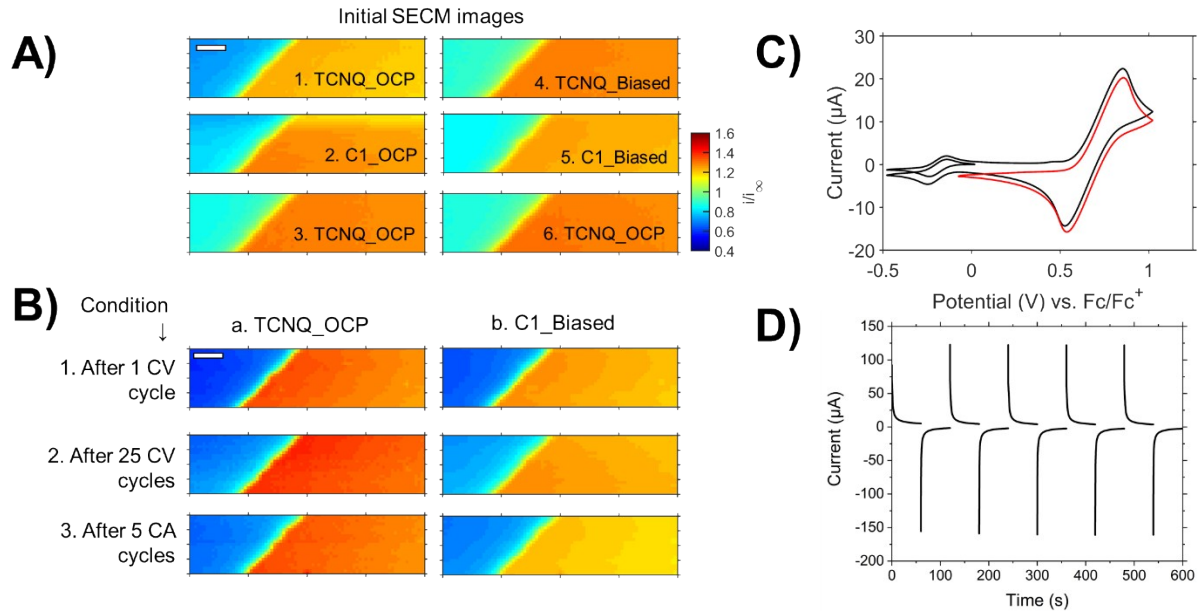

Figure S13: A) Normalized SECM images of MLG feedback using 0.5 mM TCNQ and 5 mM C1 as redox mediators with 0.1 M $LiBF_4$ in PC before any conditioning; image scale bar is 20 µm. Images were taken with substrate electrode: (i) at OCP using TCNQ, (ii) at OCP using C1, (iii) at OCP using TCNQ, (iv) biased at -0.08 V vs Fc/Fc^+ using TCNQ, (v) biased at -0.08 V vs. Fc/Fc^+ using C1, and (vi) at OCP using C1. The probe was biased to -0.43 V vs Fc/Fc^+ for TCNQ imaging and 0.97 V vs. Fc/Fc^+ for C1 imaging. B) SECM images of MLG feedback following conditioning steps using TCNQ and C1 solutions mentioned above; image scale bar is 20 µm. Images were taken with the substrate electrode: (i) after one substrate CV, (ii) after 25 more substrate CVs, and (iii) after five sets of oxidative then reductive chronoamperograms. The probe was biased as mentioned above and the substrate was either at (a) OCP or (b) biased to -0.08 V vs. Fc/Fc^+. C) Cyclic voltammograms with MLG Substrate. The black trace is the first cycle of both TCNQ and C1, and red trace is the 26^{th} total cycle showing C1 only. D) Chronoamperometry with MLG substrate using an oxidation potential of 1.02 V vs. Fc/Fc^+ and reduction potential of -0.08 V vs. Fc/Fc^+.

IV. Filming on MLG

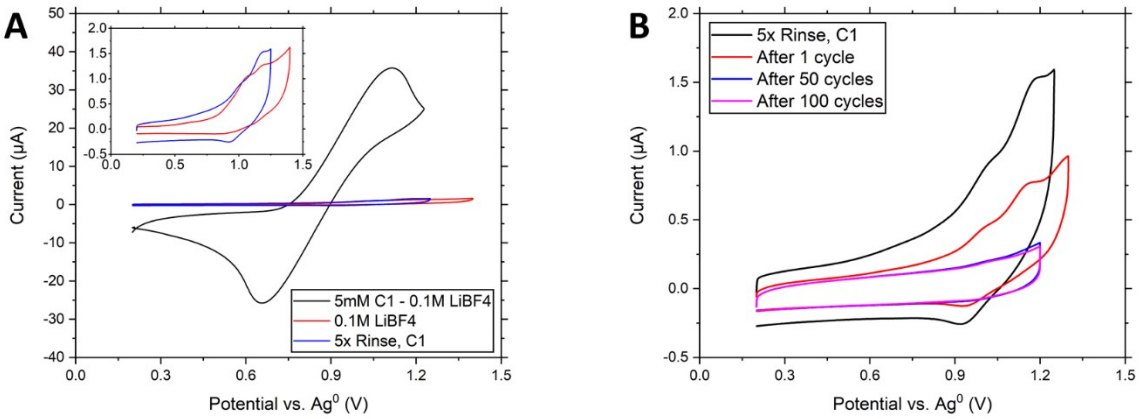

A. C1 Filming

Figure S14: A) CVs with a MLG substrate in 5 mM C1 with 0.1 M $LiBF_4$ in PC (black trace), in 0.1 M $LiBF_4$ before any addition of C1 (red trace), and after 25 CVs and 5 CAs in 5 mM C1 with 0.1 M $LiBF_4$ and rinsing five times with PC (blue trace). Inset shows zoom in of red and blue traces. B) Multiple consecutive CVs of the sample following the cycling and rinsing mentioned above for the blue trace. The decline in current indicates that any redox active film, if formed at all, desorbs from surface over time or with repetitive cycling.

B. C7 Filming

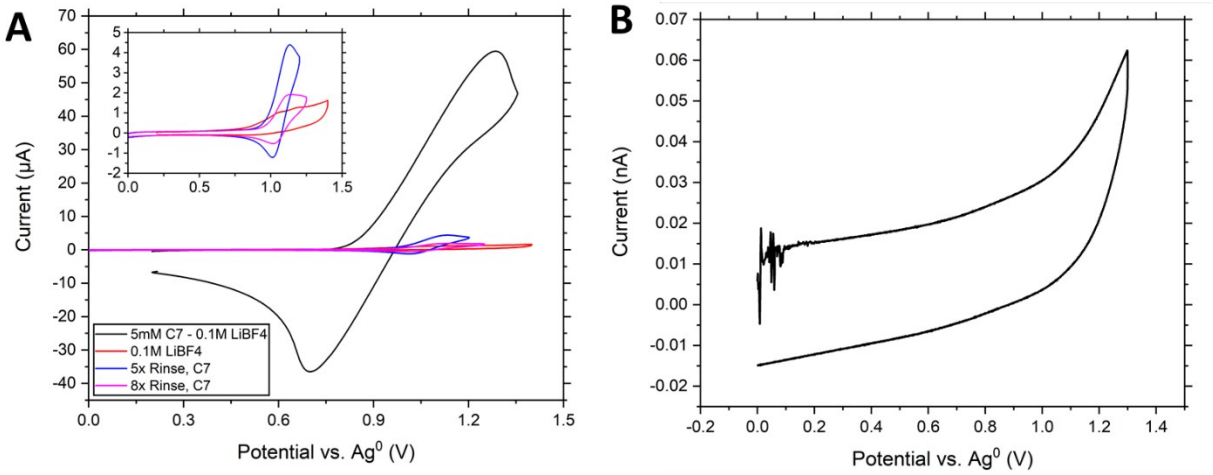

Figure S15: A) CVs with a MLG substrate: in 5 mM C7 with 0.1 M $LiBF_4$ in PC (black trace), in 0.1 M $LiBF_4$ before any addition of C7 (red trace), after 25 CVs and 5 CAs in 5 mM C7 with 0.1 M $LiBF_4$ and rinsing five times with PC (blue trace), and after rinsing with PC a total of eight times (magenta trace). Inset shows zoom in of red, blue, and magenta traces. B) Cyclic voltammogram with an UME placed in PC approximately 1-2 mm from MLG substrate after eighth serial rinse.

No faradaic signal was observed in the region anticipated for C7, which indicated the absence of solvated C7 in the post-washing MLG electrochemistry.

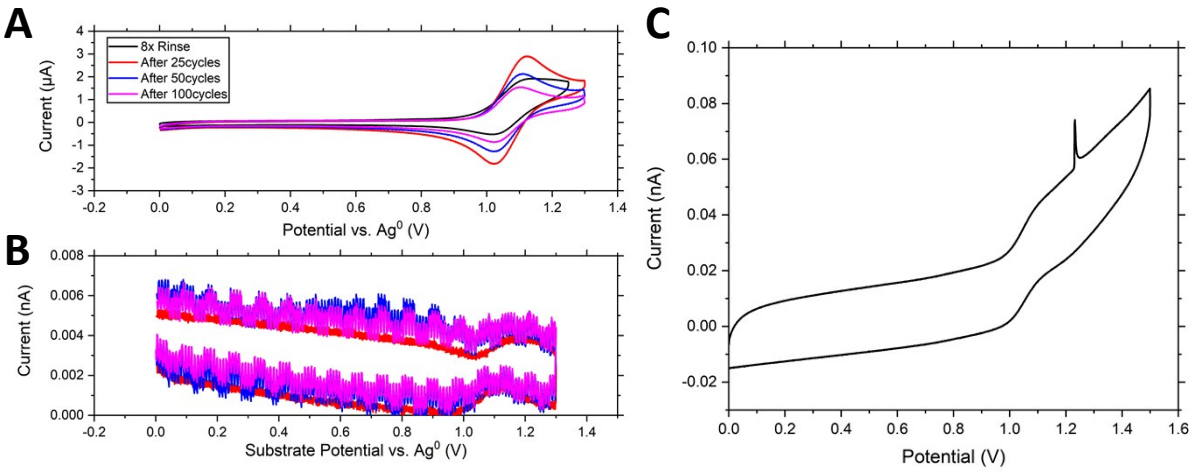

Figure S16: A) Cyclc voltammetry of conditioned MLG sample in 0.1 M $LiBF_4$ and PC after rinsing procedure described in figure S15. The black trace represents MLG substrate after eighth serial rinse, the red trace is after a total of 25 cycles, the blue trace is after a total of 50 cycles, and the magenta trace is after a total of 100 cycles. B) UME placed above MLG substrate and biased to 0 V vs. Ag^0 to collect any oxidized products generated during the MLG CVs in figure S16A. A small faradaic signal was observed when the substrate potential reached 1.1 V vs Ag^0. C) UME CV after cycling the substrate for 100 times and resting the substrate for approximately 10 h. Comparing this UME CV with a faradaic component to the initial CV where the UME was placed in solution, figure S15B, strongly indicates the presence of a desorbed redox active species in solution that was not detected earlier.

V. AFM C1 vs C7

A. HOPG baseline

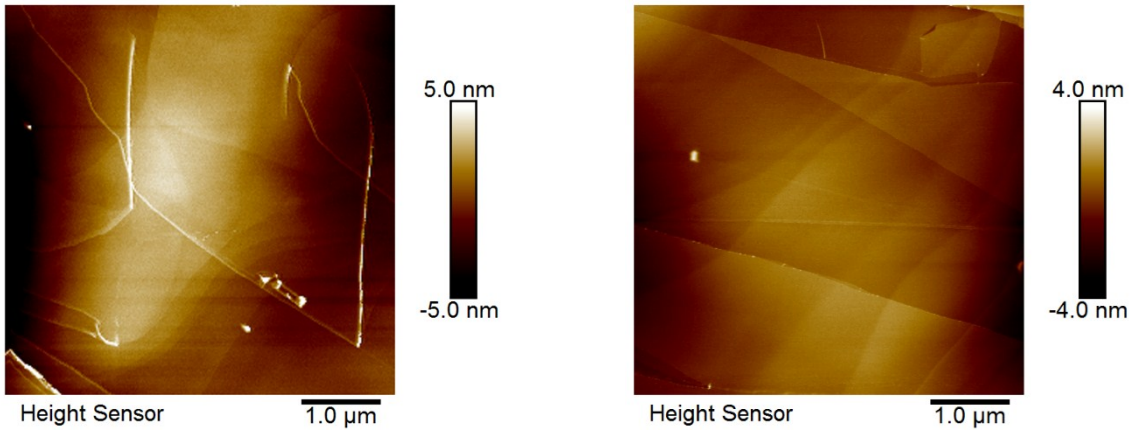

Figure S17: AFM images of HOPG substrates, in their dry states, used in to collect the *in situ* data shown in Figure 2a (left) and Figure 2e (right) of the main text. These images emphasize the pristine nature of a freshly cleaved HOPG surface—in contrast to the often-observed low density scattering of particles when the surface is first immersed in the electrolyte.

B. Nanomechanical Property Maps:

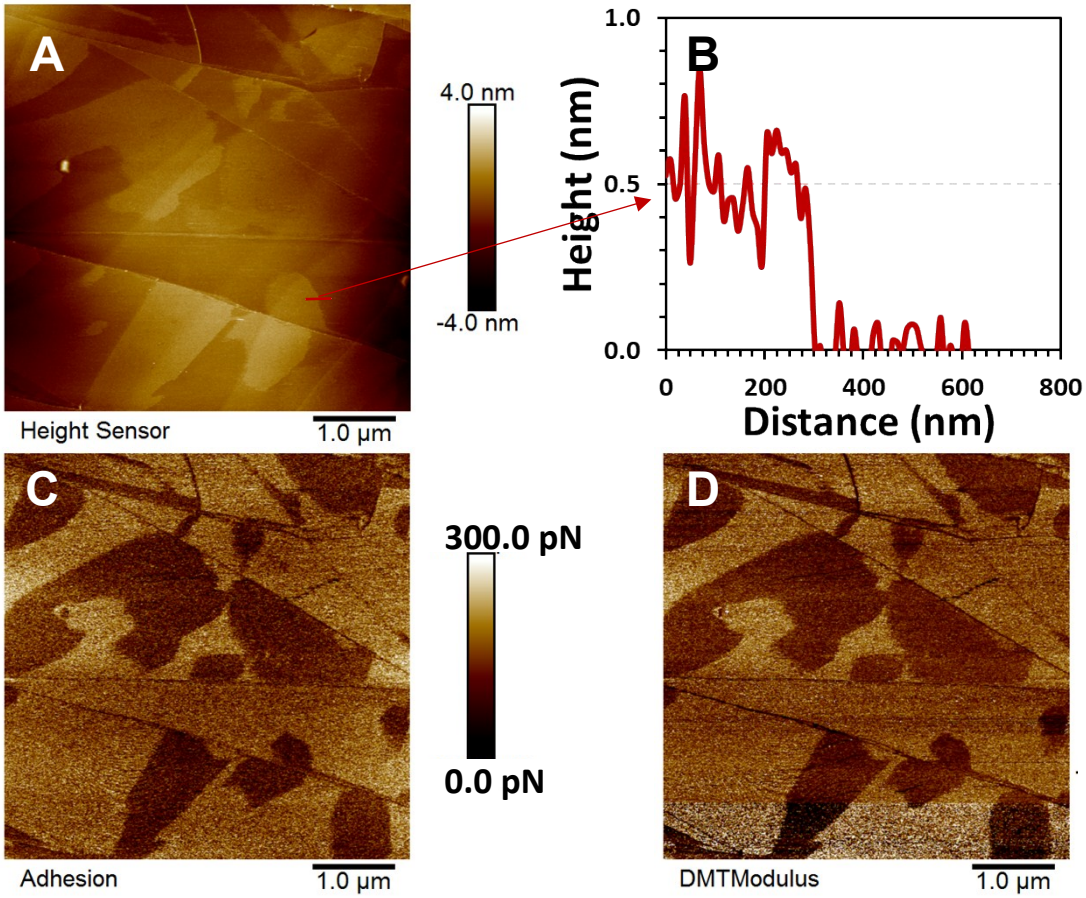

Figure S18: Nanomechanical property maps of film formation during the reduction of $C7^{+\bullet}$ asdiscussed in Figure 2G; A) Topographic image of film formation, B) Topographic profile showing a 0.5 nm film thickness, C) Relative adhesive force between the material and the tip, and D) Relative elastic modulus(Derjaguin, Muller, Toropov model).

C. Li Reference Electrode Contamination:

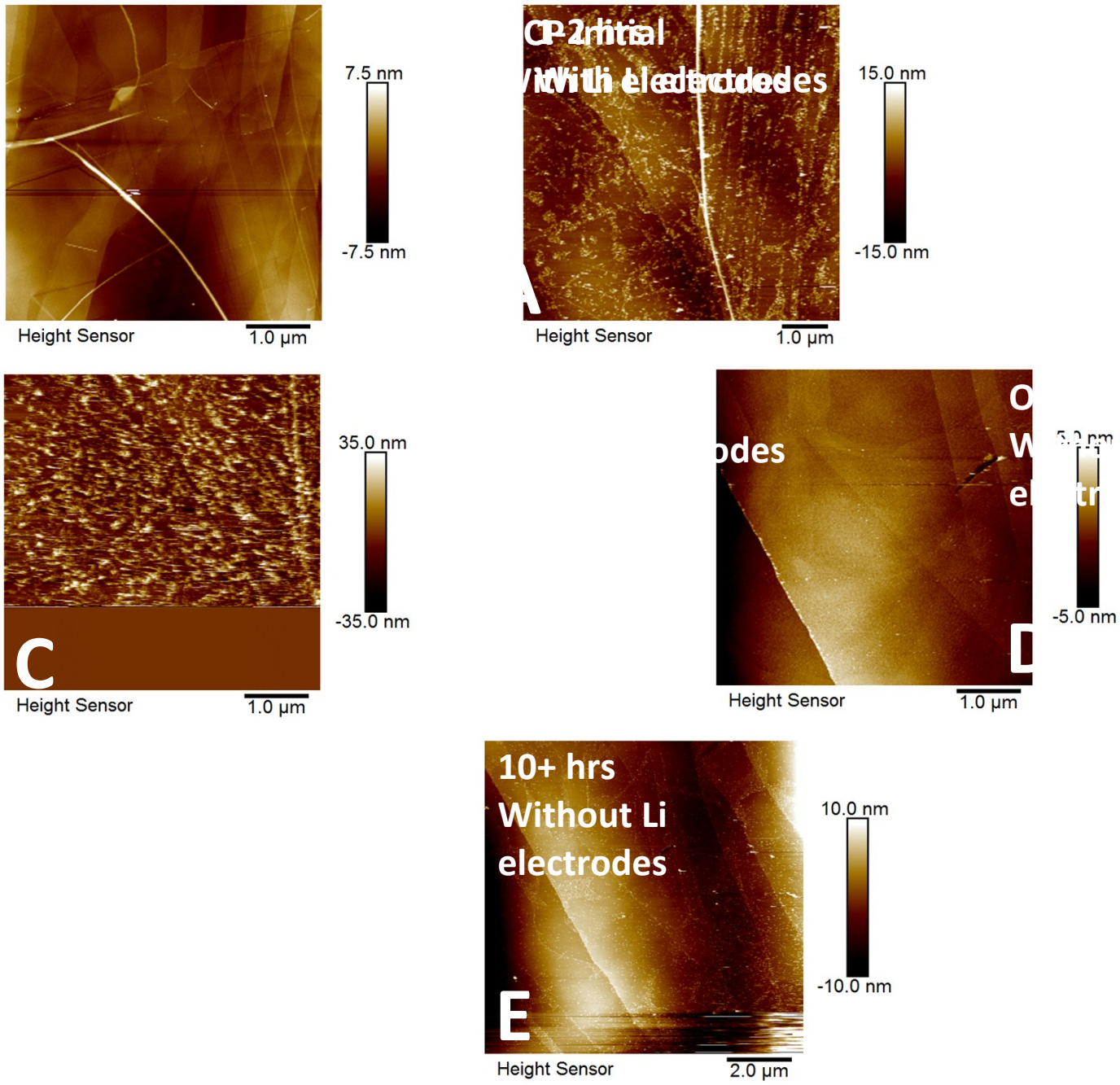

Figure S19: Open Circuit images, immediately after cell assembly (A) through 10+ hours (C) with 5 mM C1 + 0.1 M $LiBF_4$/PC electrolyte sitting over HOPG with Li CE and RE present. Open circuit images, immediately after assembly (D) and 10+ hours (E) with the same electrolyte but the absence of Li electrodes. (This data is intended to highlight the problem of particle generation when using metallic Li as electrodes.)

VI. SECM: SLG vs. HOPG Edge

A. C1 SLG Substrate in $LiBF_4$

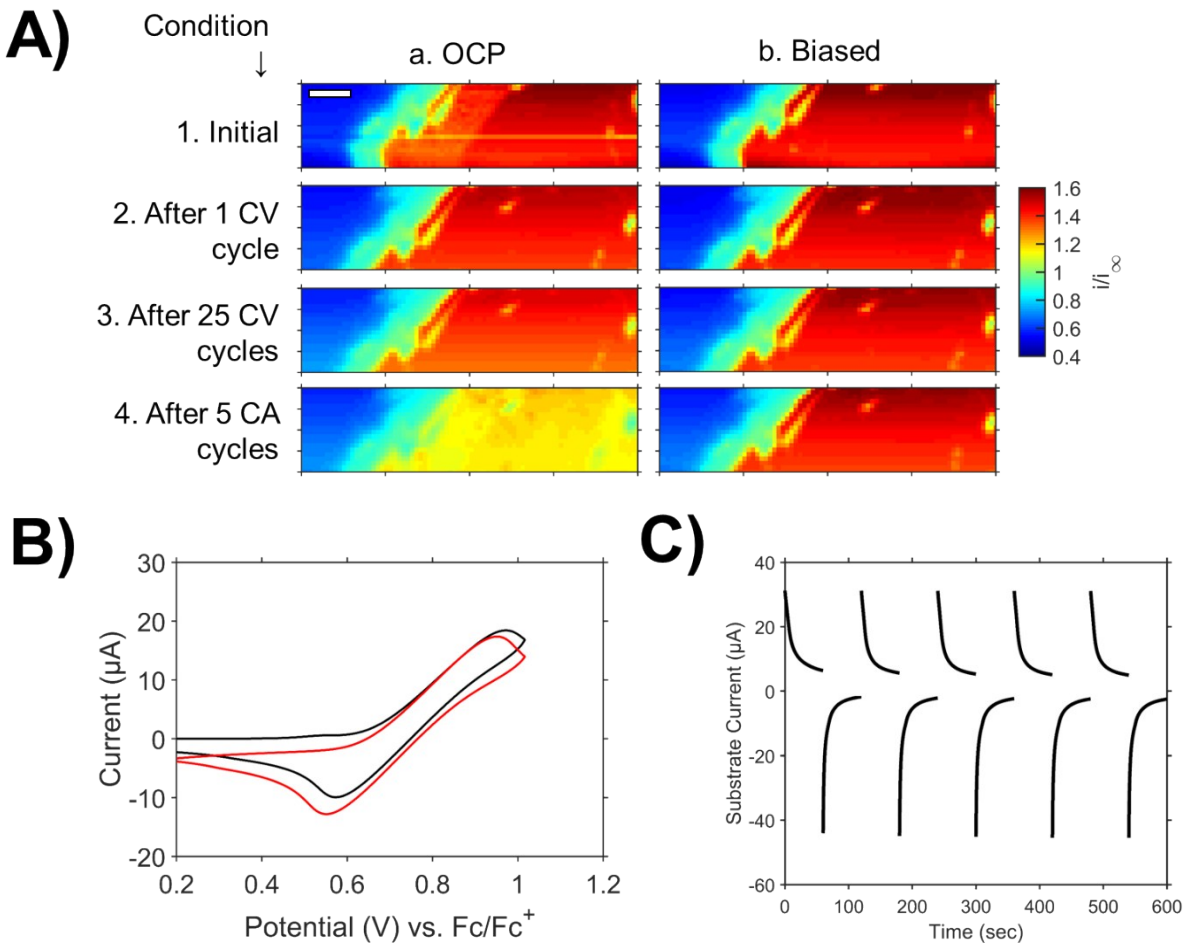

Figure S20: A) Normalized SECM images of a SLG electrode using 5 mM C1 catholyte mediator in 0.1 M $LiBF_4$ electrolyte in PC; image scale bars are 20 μm. Images were taken with the substrate electrode: (i) at the initial condition before substrate biasing, (ii) after one substrate CV, (iii) after 25 more substrate CVs, and (iv) after five sets of oxidative then reductive chronoamperograms. The probe was biased at 0.97 V vs. Fc/Fc^+, and the substrate was either at a) OCP or b) biased to -0.18 V vs. Fc/Fc^+. B) Cyclic voltammograms with a SLG substrate. The black trace is the first cycle and red trace is the 26th total cycle. C) Chronoamperometry with SLG substrate using an oxidation potential of 1.02 V vs. Fc/Fc^+ and reduction potential of -0.18 V vs Fc/Fc^+.

B. C7 SLG Substrate in $LiBF_4$

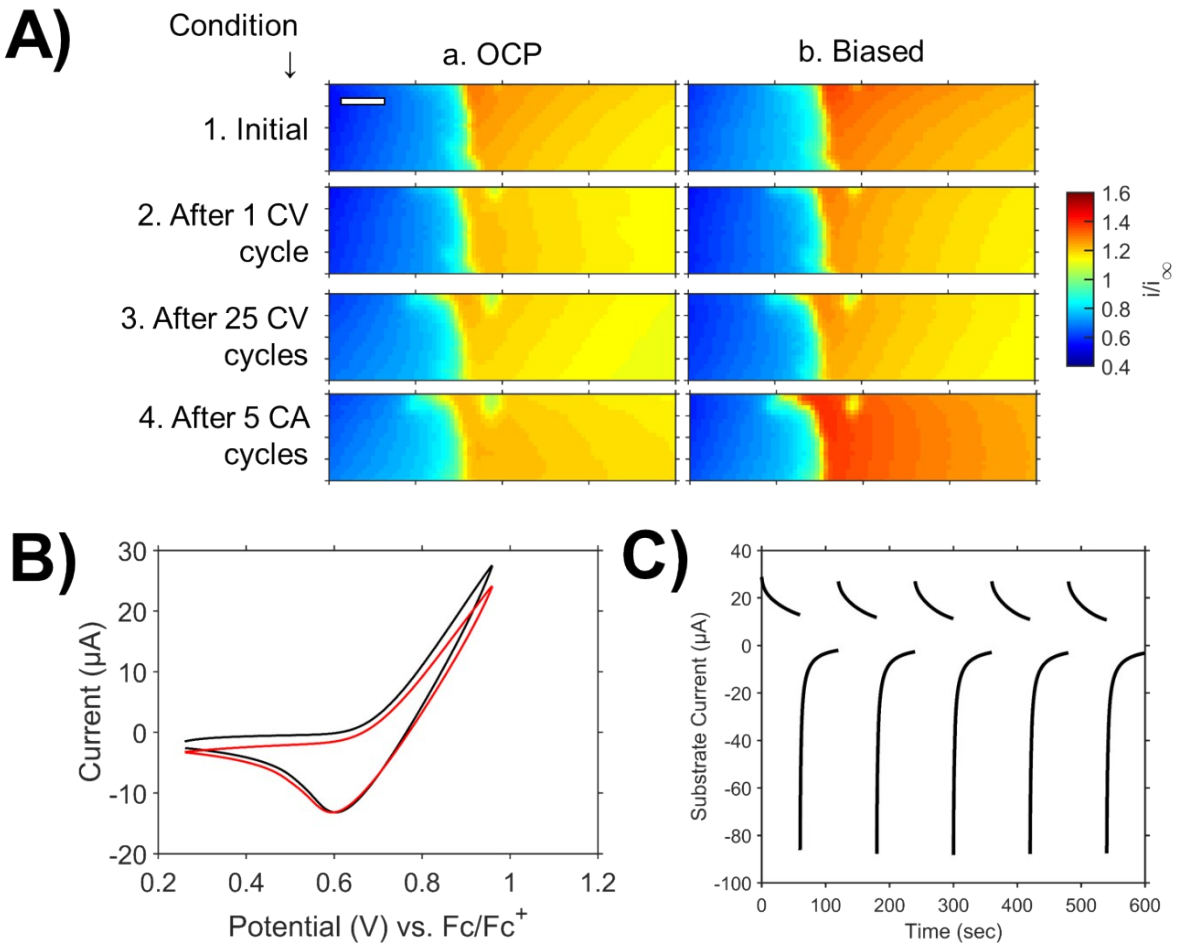

Figure S21: A) Normalized SECM images of a SLG electrode using 5 mM C7 catholyte mediator in 0.1 M $LiBF_4$ electrolyte in PC; image scale bars are 20 μm. Images were taken with the substrate electrode: (i) at the initial condition before substrate biasing, (ii) after one substrate CV, (iii) after 25 more substrate CVs, and (iv) after five sets of oxidative then reductive chronoamperograms. The probe was biased at 0.96 V vs. Fc/Fc^+, and the substrate was either at a) OCP or b) biased to -0.24 V vs. Fc/Fc^+. B) Cyclic voltammograms with a SLG substrate. The black trace is the first cycle and red trace is the 26th total cycle. C) Chronoamperometry with SLG substrate using an oxidation potential of 0.96 V vs. Fc/Fc^+ and reduction potential of -0.24 V vs. Fc/Fc^+.

C. C1 HOPG Edge Substrate in $LiBF_4$

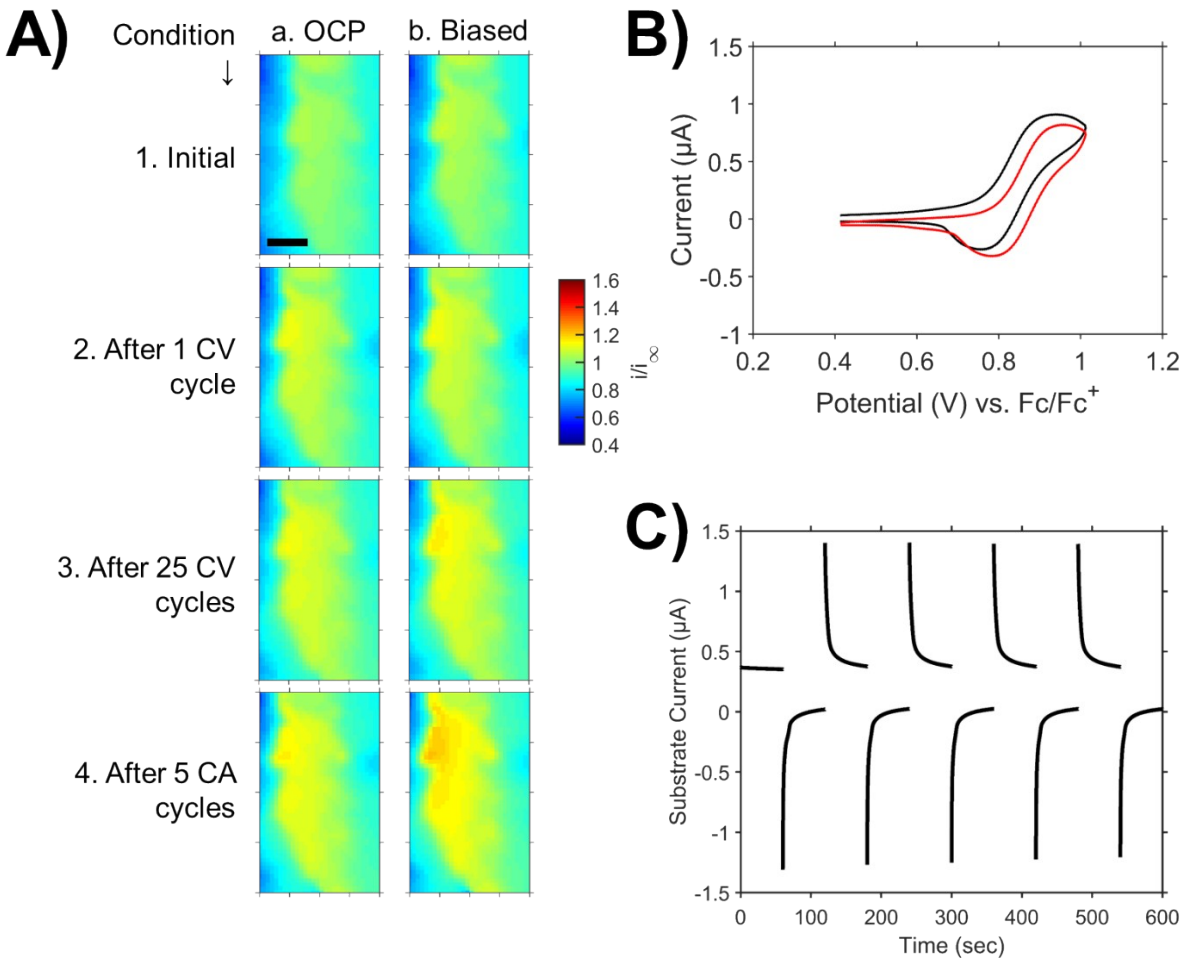

Figure S22: A) Normalized SECM images of a HOPG edge electrode using 5 mM C1 catholyte mediator in 0.1 M $LiBF_4$ electrolyte in PC; image scale bars are 20 μm. Images were taken with the substrate electrode: (i) at the initial condition before substrate biasing, (ii) after one substrate CV, (iii) after 25 more substrate CVs, and (iv) after five sets of oxidative then reductive chronoamperograms. The probe was biased at 1.01 V vs. Fc/Fc^+, and the substrate was either at a) OCP or b) biased to -0.02 V vs. Fc/Fc^+. B) Cyclic voltammograms with a HOPG edge substrate. The black trace is the first cycle and red trace is the 26th total cycle. C) Chronoamperometry with HOPG edge substrate using an oxidation potential of 1.01 V vs. Fc/Fc^+ and reduction potential of 0.01 V vs. Fc/Fc^+.

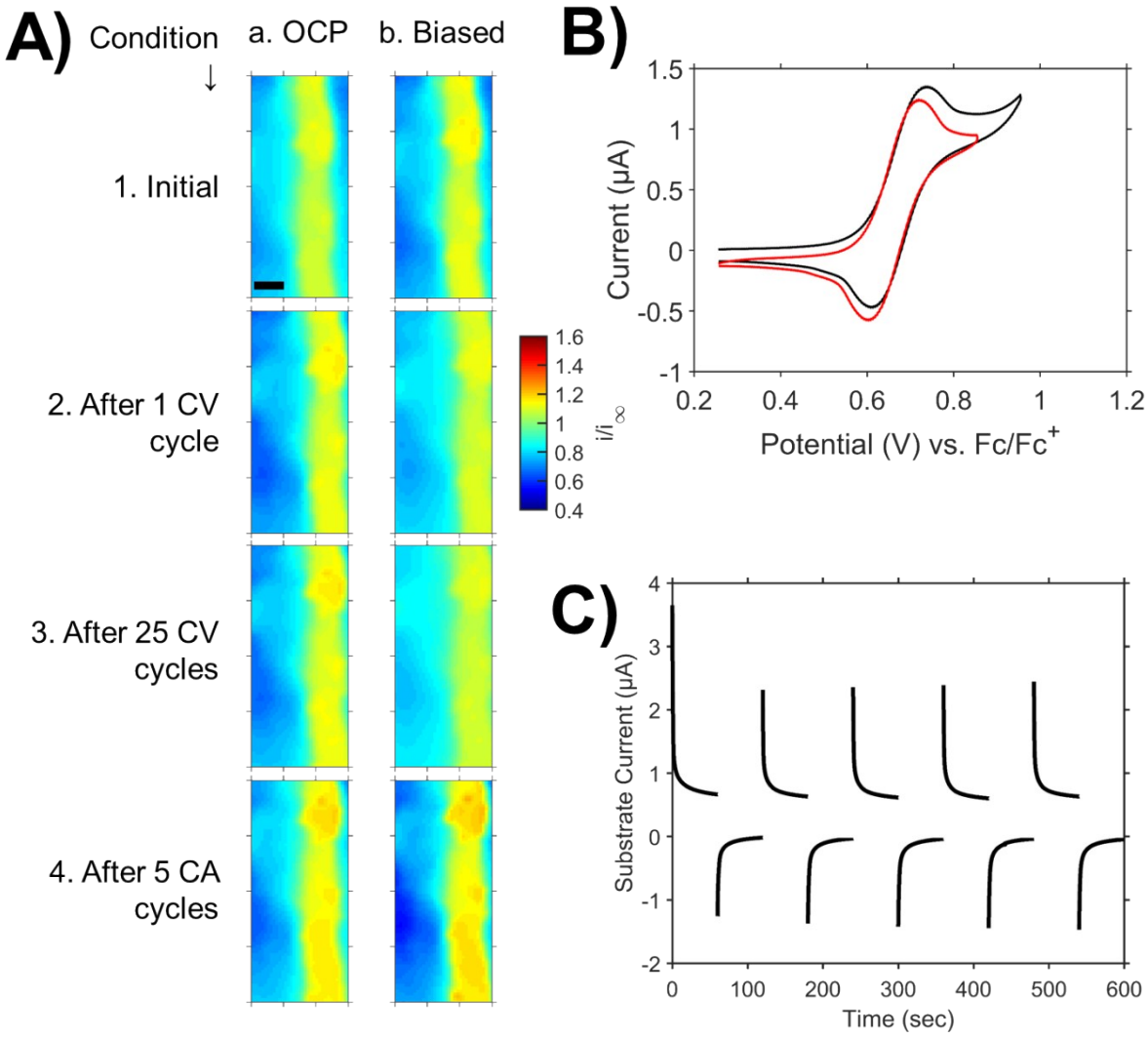

D. C7 HOPG Edge Substrate in $LiBF_4$

Figure S23: A) Normalized SECM images of a HOPG edge electrode using 5 mM C7 catholyte mediator in 0.1 M $LiBF_4$ electrolyte in PC; image scale bars are 20 μm. Images were taken with the substrate electrode: (i) at the initial condition before substrate biasing, (ii) after one substrate CV, (iii) after 25 more substrate CVs, and (iv) after five sets of oxidative then reductive chronoamperograms. The probe was biased at 0.96 V vs. Fc/Fc^+, and the substrate was either at a) OCP or b) biased to -0.35 V vs. Fc/Fc^+. B) Cyclic voltammograms with a HOPG edge substrate. The black trace is the first cycle and red trace is the 26th total cycle. C) Chronoamperometry with HOPG edge substrate using an oxidation potential of 0.86 V vs. Fc/Fc^+ and reduction potential of -0.35 V vs. Fc/Fc^+.

E. C1 + TCNQ + HOPG Basal Plane

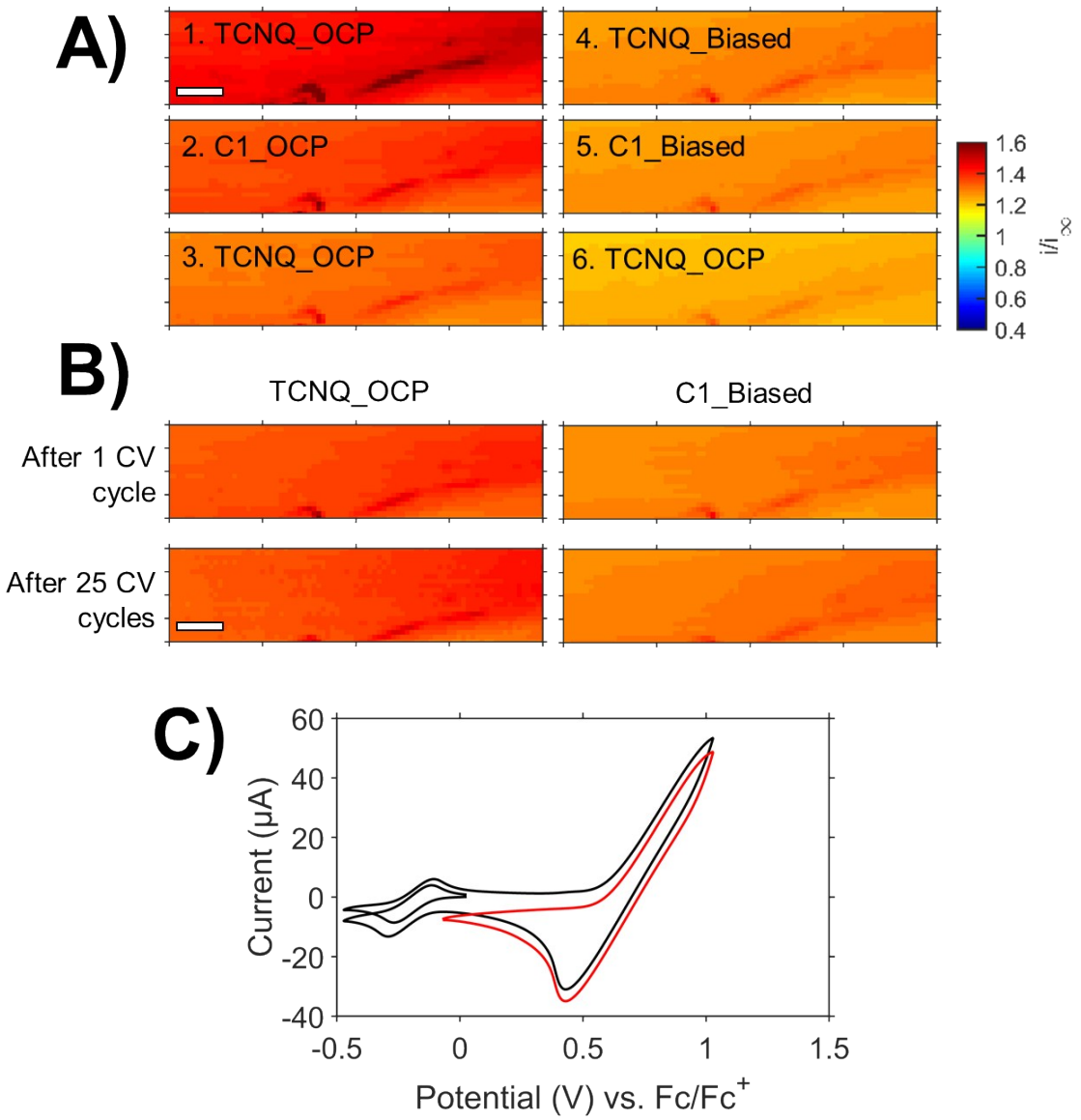

Figure S24: A) Normalized SECM images of HOPG basal plane feedback using 0.5 mM TCNQ and 5 mM C1 as redox mediators with 0.1 M $LiBF_4$ in PC before any conditioning; image scale bar is 20 µm. Images were taken with substrate electrode: (i) at OCP using TCNQ, (ii) at OCP using C1, (iii) at OCP using TCNQ, (iv) biased at -0.06 V vs Fc/Fc^+ using TCNQ, (v) biased at -0.06 V vs. Fc/Fc^+ using C1, and (vi) at OCP using C1. The probe was biased to -0.41 V vs Fc/Fc^+ for TCNQ imaging and 0.99 V vs. Fc/Fc^+ for C1 imaging. B) SECM images of HOPG basal plane feedback following conditioning steps using TCNQ and C1 solutions mentioned above; image scale bar is 20 µm. Images were taken with the substrate electrode: (i) after one substrate CV, (ii) after 25 more substrate CVs. The probe was biased as mentioned above and the substrate was either at (a) OCP or (b) biased to -0.06 V vs. Fc/Fc^+. C) Cyclic voltammograms with MLG

Substrate. The black trace is the first cycle of both TCNQ and C1, and red trace is the 26th total cycle showing C1 only.

VII. SECM: LiTFSI

A. C1 MLG Substrate

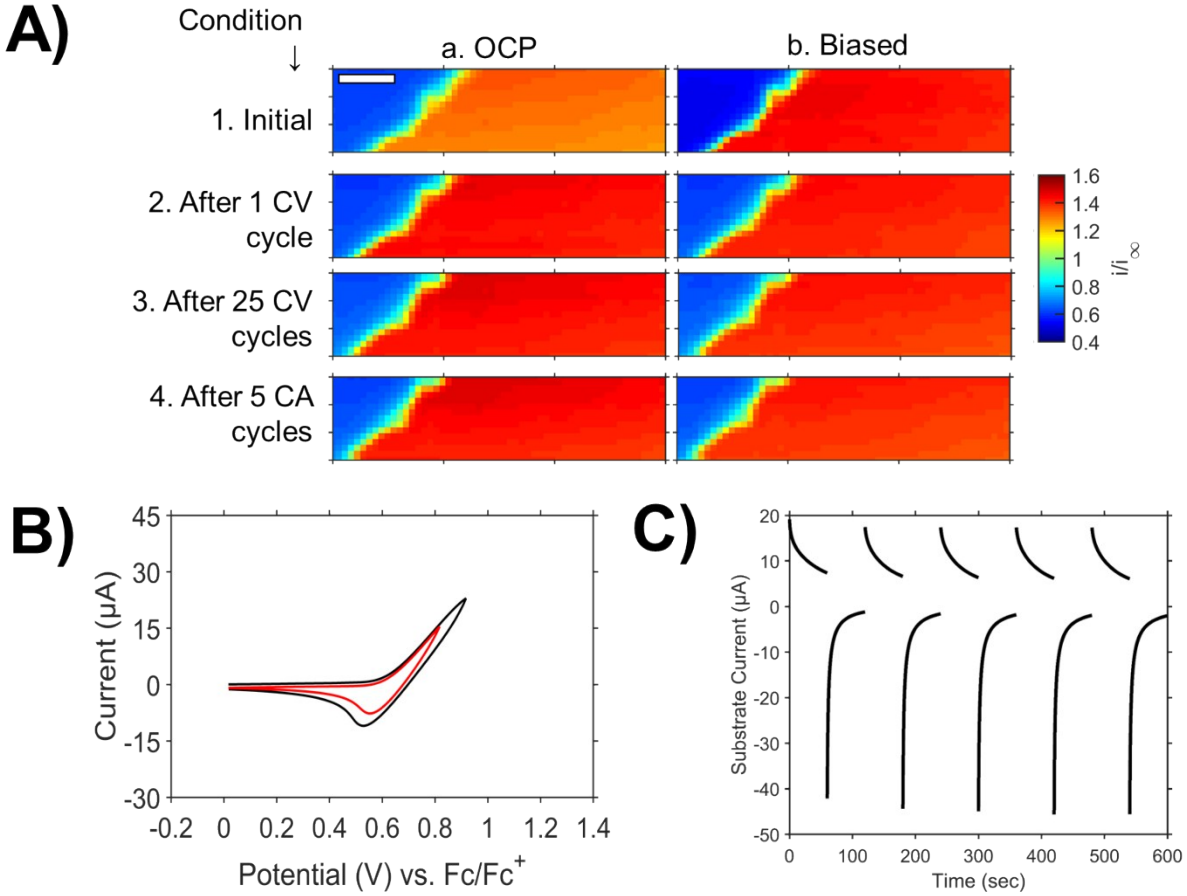

Figure S25: A) Normalized SECM images of a MLG electrode using 5 mM C1 as catholyte mediator in 0.1 M LiTFSI electrolyte in PC; image scale bars are 20 μm. Images were taken with the substrate electrode: (i) at the initial condition before substrate biasing, (ii) after one substrate CV, (iii) after 25 more substrate CVs, and (iv) after five sets of oxidative then reductive chronoamperograms. The probe was biased at 0.92 V vs. Fc/Fc^+, and the substrate was either at a) OCP or b) biased to -0.48 V vs. Fc/Fc^+. B) Cyclic voltammograms with the MLG substrate. The black trace is the first cycle and red trace is the 26th total cycle. C) Chronoamperometry with MLG substrate using an oxidation potential of 0.82 V vs. Fc/Fc^+ and reduction potential of -0.48 V vs Fc/Fc^+.

B. C7 MLG Substrate

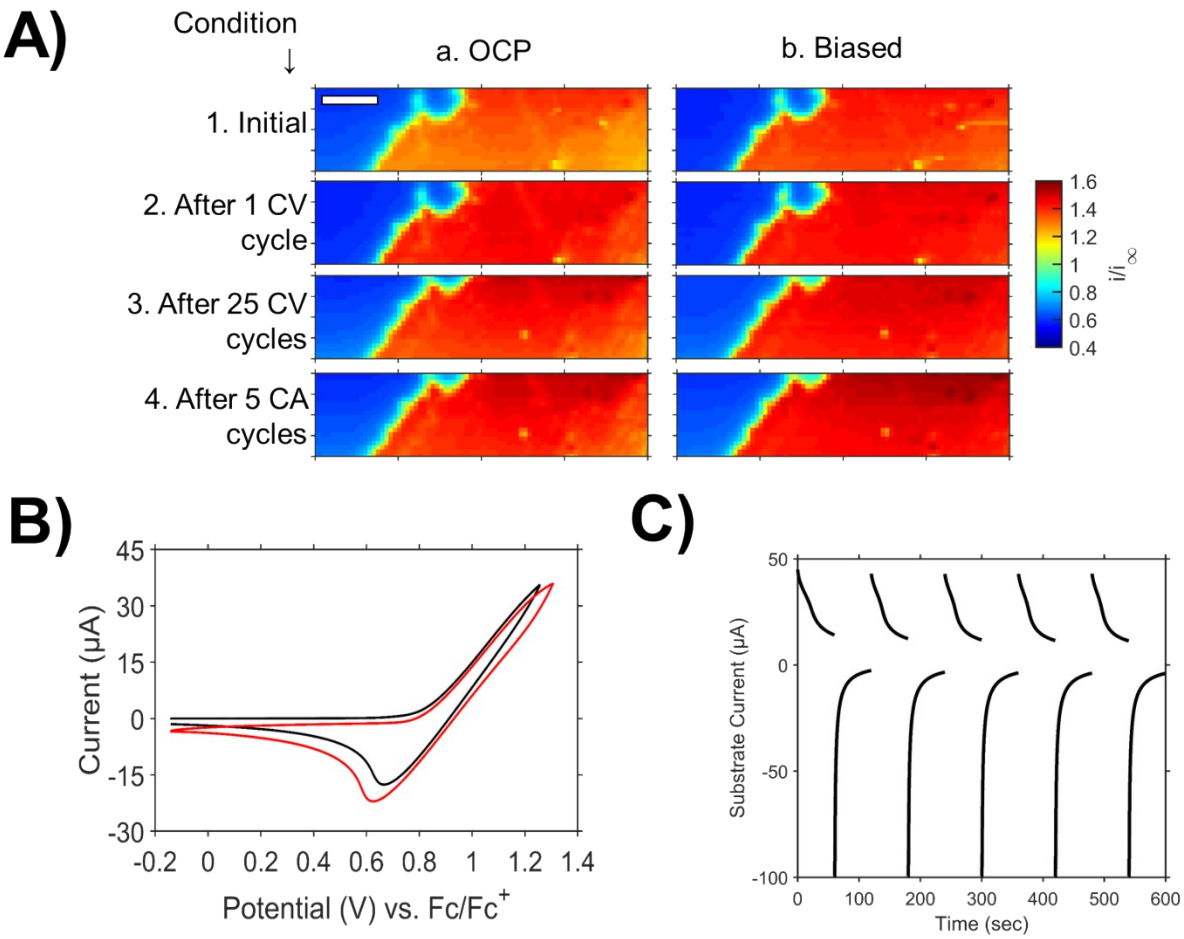

Figure S26: A) Normalized SECM images of a MLG electrode using 5 mM C7 as catholyte mediator in 0.1 M LiTFSI electrolyte in PC; image scale bars are 20 μm. Images were taken with the substrate electrode: (i) at the initial condition before substrate biasing, (ii) after one substrate CV, (iii) after 25 more substrate CVs, and (iv) after five sets of oxidative then reductive chronoamperograms. The probe was biased at 1.21 V vs. Fc/Fc^+, and the substrate was either at a) OCP or b) biased to -0.14 V vs. Fc/Fc^+. B) Cyclic voltammograms with the MLG substrate. The black trace is the first cycle and red trace is the 26^{th} total cycle. C) Chronoamperometry with MLG substrate using an oxidation potential of 1.26 V vs. Fc/Fc^+ and reduction potential of -0.14 V vs. Fc/Fc^+.

VIII. AFM: LiTFSI

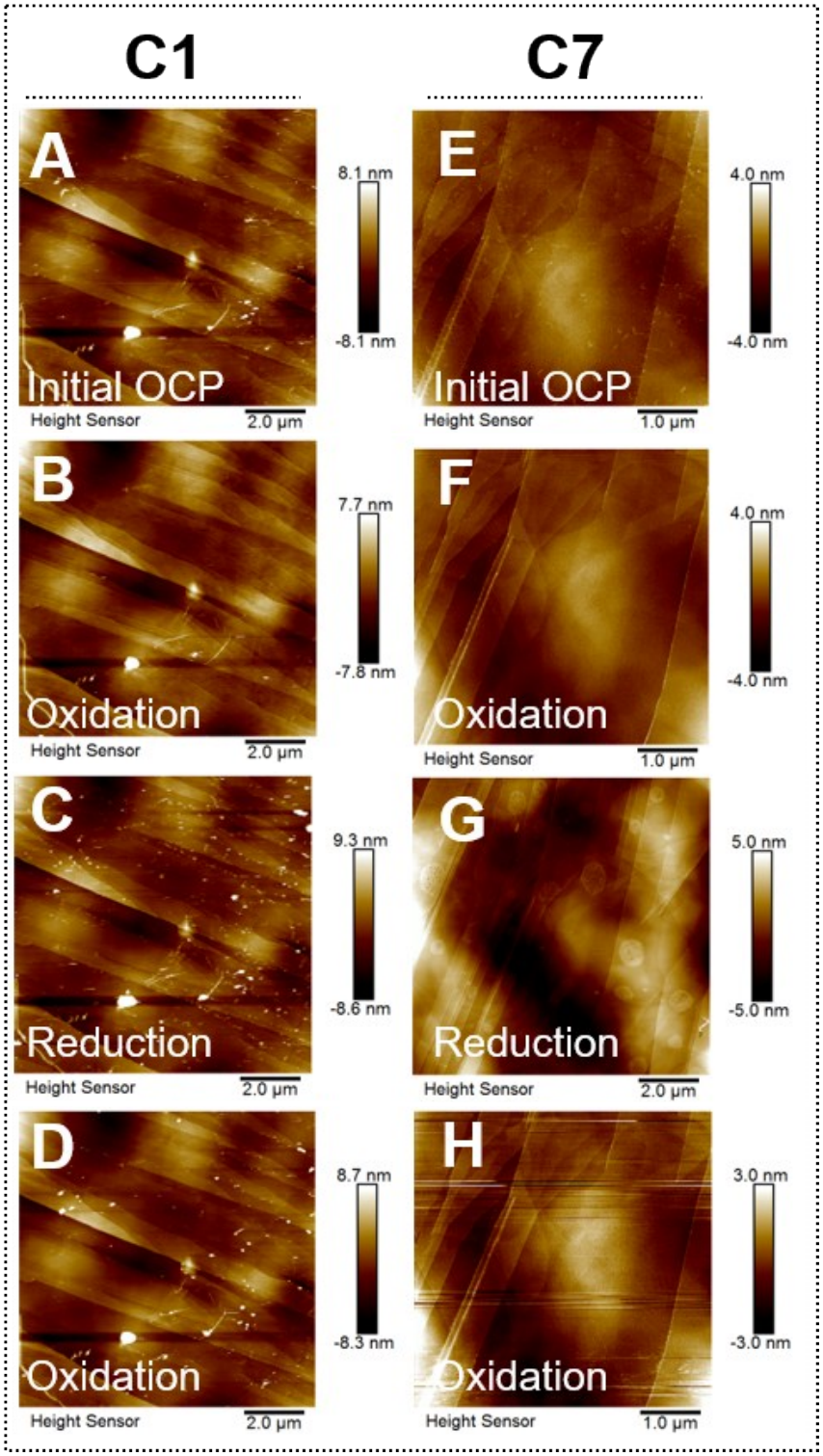

Figure S27: *In situ* AFM images of the HOPG surface during experiments equivalent to those in Figure 2a-h of the main text, but with LiTFSI as the supporting salt. Figure S27G is equivalent to Figure 4F in the main text.

IX. SECM k_f Quantification

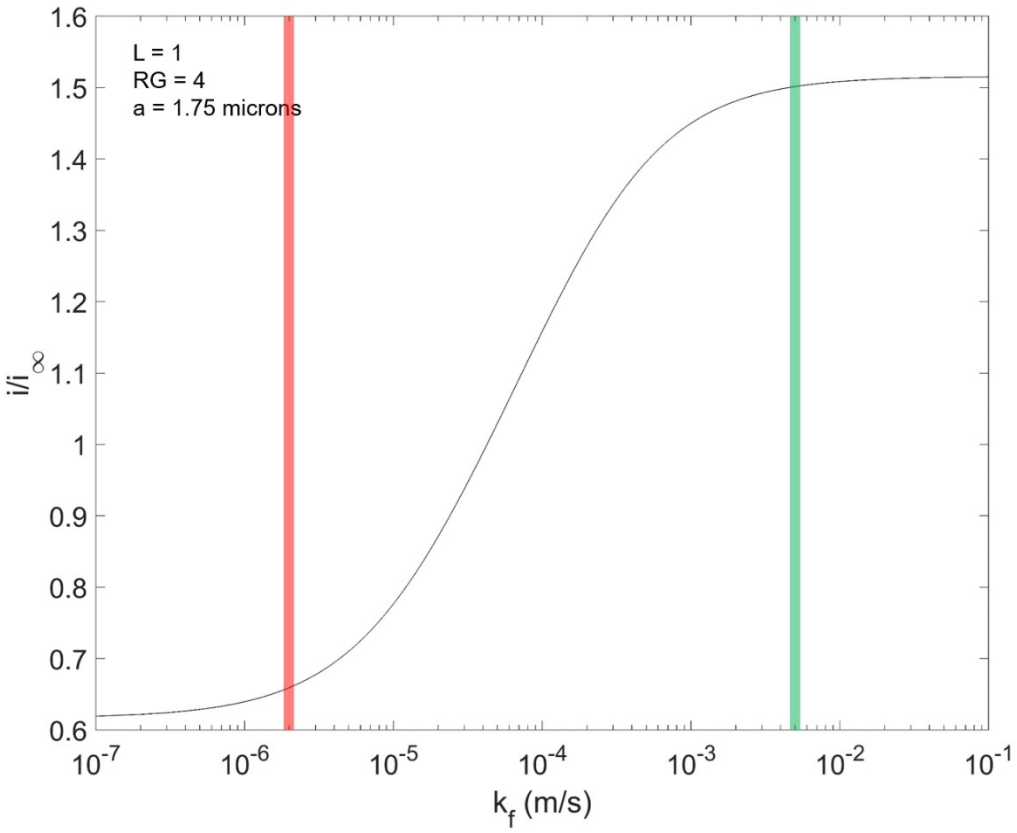

Figure S28. Theoretical plot of normalized tip currents versus the calculated k_f from the given tip geometry and tip-substrate distance that was used in this work. The red and green lines correspond to the upper and lower limits of quantitation given in the main text.

X. Summary of SECM Experiments

	C1	C7
MLG with $LiBF_4$	Relevant Figures: Fig. 1, S11	Relevant Figures: Fig. 1, S12
	kf at OCP (m/s) = 1.3×10^{-4} (initial), 2.5×10^{-4} (final)	kf at OCP (m/s) = 1.3×10^{-4} (initial), 1.6×10^{-4} (final)
	kf at Biased (m/s) = 1.8×10^{-4} (initial), 5×10^{-3} (final)	kf at Biased (m/s) = 2.9×10^{-4} (initial), 1.4×10^{-4} (final)
MLG with LiTFSI	Relevant Figures: Fig. 4, S25	Relevant Figures: Fig. 4, S26
	kf at OCP (m/s) = 1.3×10^{-4} (initial), 3.6×10^{-4} (final)	kf at OCP (m/s) = 3.1×10^{-4} (initial), 9.8×10^{-4} (final)
	kf at Biased (m/s) = 3.6×10^{-4} (initial), 2.3×10^{-4} (final)	kf at Biased (m/s) = 5.5×10^{-4} (initial), 3.1×10^{-3} (final)
SLG	Relevant Figures: Fig. 3, S20	Relevant Figures: Fig. 3, S21
	kf at OCP (m/s) = 4.6×10^{-4} (initial), 5.3×10^{-5} (final)	kf at OCP (m/s) = 1.3×10^{-4} (initial), 1.3×10^{-4} (final)
	kf at Biased (m/s) = 7.1 × 10-4 (initial), 3.8×10^{-4} (final)	kf at Biased (m/s) = 1.8×10^{-4} (initial), 2.4×10^{-4} (final)
HOPG Edge	Relevant Figures: Fig. 3, S22	Relevant Figures: Fig. 3, S23
	kf at OCP (m/s) = 1.4×10^{-5} (initial), 2.9×10^{-5} (final)	kf at OCP (m/s) = 6.4×10^{-5} (initial), 3.1×10^{-4} (final)
	kf at Biased (m/s) = 1.8×10^{-5} (initial), 5.5×10^{-5} (final)	kf at Biased (m/s) = 9.9×10^{-5} (initial), 5.9×10^{-4} (final)

Table S1. Summary of SECM experiments with C1 and C7 catholytes with various substrates and supporting electrolytes. The reported k_f values are median values, where "initial" is the image taken before any substrate cycling and "final" is the image taken after 26 total CVs and 5 CA sets as described in the relevant figures and main text.

XI. References

1 J. Hui, M. Burgess, J. Zhang and J. Rodríguez-López, *ACS Nano*, 2016, **10**, 4248–4257.

2 J. Hui, N. B. Schorr, S. Pakhira, Z. Qu, J. L. Mendoza-Cortes and J. Rodríguez-López, *J. Am. Chem. Soc.*, 2018, **140**, 13599–13603.

3 J. D. Wood, G. P. Doidge, E. A. Carrion, J. C. Koepke, J. A. Kaitz, I. Datye, A. Behnam, J. Hewaparakrama, B. Aruin, Y. Chen, H. Dong, R. T. Haasch, J. W. Lyding and E. Pop, *Nanotechnology*, 2015, **26**, 55302.

4 R. R. Nair, P. Blake, A. N. Grigorenko, K. S. Novoselov, T. J. Booth, T. Stauber, N. M. R. Peres and A. K. Geim, *Science (80-.).*, 2008, **320**, 1308 LP – 1308.

5 S. Bhaviripudi, X. Jia, M. S. Dresselhaus and J. Kong, *Nano Lett.*, 2010, **10**, 4128–4133.

6 Z. T. Gossage, J. Hui, Y. Zeng, H. Flores-Zuleta and J. Rodríguez-López, *Chem. Sci.*, 2019, **10**, 10749–10754.

7 C. Lefrou and R. Cornut, *ChemPhysChem*, 2010, **11**, 547–556.

8 J. Ghilane, P. Hapiot and A. J. Bard, *Anal. Chem.*, 2006, **78**, 6868–6872.